AGU PUBLICATIONS

Geophysical Research Letters

RESEARCH LETTER
10.1002/2016GL068363

Key Points:
- The first kinetic simulation of jovian plasma and energetic particle interaction with Ganymede's magnetosphere
- Correlation between energetic ion precipitation to the surface of Ganymede and Ganymede's surface brightness
- Energetic ion precipitation to Ganymede's surface peaks near 100–300 keV

Correspondence to:
S. Fatemi,
shahab@ssl.berkeley.edu

Citation:
Fatemi, S., A. R. Poppe, K. K. Khurana, M. Holmström, and G. T. Delory (2016), On the formation of Ganymede's surface brightness asymmetries: Kinetic simulations of Ganymede's magnetosphere, *Geophys. Res. Lett.*, *43*, doi:10.1002/2016GL068363.

Received 19 FEB 2016
Accepted 14 APR 2016
Accepted article online 30 APR 2016

On the formation of Ganymede's surface brightness asymmetries: Kinetic simulations of Ganymede's magnetosphere

S. Fatemi[1], A. R. Poppe[1], K. K. Khurana[2], M. Holmström[3], and G. T. Delory[1]

[1]Space Sciences Laboratory, University of California, Berkeley, California, USA, [2]Institute of Geophysics and Planetary Physics, University of California, Los Angeles, California, USA, [3]Swedish Institute of Space Physics, Kiruna, Sweden

Abstract Ganymede possesses strong surface brightness asymmetries both between its polar cap and equatorial regions and between its leading and trailing hemispheres. Here we test the hypothesis that these asymmetries are due to differential Jovian plasma and energetic particle precipitation to the surface with the combination of a hybrid plasma model (kinetic ions and fluid electrons) and a particle tracing model. We describe the hybrid model, the first of its kind applied to Ganymede, and compare the results to both Galileo observations and previous MHD and MHD-EPIC models of Ganymede. We calculate spatially resolved precipitating Jovian ion fluxes to the surface of Ganymede for energies $1 < E < 10^4$ keV and find (1) precipitating fluxes peak near 100 keV and (2) excellent correlation between the precipitating flux and Ganymede's surface brightness variations. Thus, we conclude that precipitating energetic particle fluxes are the primary driver for altering the surface brightness of Ganymede.

1. Introduction

Ganymede, the largest Galilean moon of Jupiter and the largest moon of our solar system, is the only known moon that has its own intrinsic magnetic field [*Gurnett et al.*, 1996; *Kivelson et al.*, 1996]. The magnetic moment of Ganymede is large enough to form an embedded minimagnetosphere within the magnetosphere of Jupiter [*Kivelson et al.*, 1996, 1998]. Similar to the other Galilean moons, the Keplerian orbital speed of Ganymede around Jupiter is much slower than the speed of the Jovian corotating plasma [e.g., *Eviatar et al.*, 1998; *Neubauer*, 1998]. Thus, the plasma continually overtakes the orbital trailing hemisphere (upstream) of Ganymede [*Kivelson et al.*, 2004]. Moreover, Ganymede has a bound neutral atmosphere and an ionosphere, probably mostly composed of oxygen and hydrogen, that interact with the corotating plasma [*Carlson et al.*, 1973; *Frank et al.*, 1997; *Hall et al.*, 1998; *Eviatar et al.*, 2001].

The ≈10° tilt of Jupiter's magnetic dipole moment from its spin axis places Ganymede into two distinct plasma environments along its orbit around Jupiter: (1) inside the plasma sheet with higher plasma density where plasma beta is slightly higher than one and (2) outside the plasma sheet with lower plasma density where plasma beta is often smaller than one [e.g., *Volwerk et al.*, 1999; *Kivelson et al.*, 2004]. The sonic and Alfvénic Mach numbers, however, are smaller than one in both of these regions. Thus, the corotating plasma directly interacts with Ganymede's magnetosphere without being distorted by a bow shock upstream [e.g., *Neubauer*, 1998; *Volwerk et al.*, 1999]. Since the direction of the Jovian magnetic field is nearly opposite to the intrinsic magnetic field of Ganymede, magnetic reconnection takes place between the minimagnetosphere of Ganymede and the Jovian magnetic field [e.g., *Kivelson et al.*, 2004], such that Ganymede is known as a favorable magnetic reconnection site.

Ganymede's strong magnetosphere and its interaction with the Jovian magnetic field and plasma forms irregular boundaries of open and closed field lines (OCFL) [*Kivelson et al.*, 1996, 1998]. While the field lines are open at Ganymede's high latitudes and enable plasma access to Ganymede's polar caps, the closed field lines at low latitudes considerably limit the plasma access to the surface of Ganymede [*Johnson*, 1997; *Cooper et al.*, 2001]. Voyager 2 and Galileo spacecraft imaging of Ganymede's surface revealed bright polar caps and dark low latitude regions [*Smith et al.*, 1979; *Khurana et al.*, 2007], which may be a result of different plasma precipitation fluxes [*Johnson*, 1997; *Cooper et al.*, 2001; *Khurana et al.*, 2007]. Moreover, Hubble Space Telescope's ultraviolet auroral observations of Ganymede indicated a reasonable correlation between the location of the

auroral oval and the boundaries of Ganymede's surface pattern except in the northern, leading hemisphere [*McGrath et al.*, 2013]. Furthermore, there is an apparent longitudinal asymmetry in the low latitude surface brightness between the trailing (upstream) and the leading (downstream) hemispheres, where the leading hemisphere is brighter than the trailing hemisphere [*Clark et al.*, 1986; *Khurana et al.*, 2007]. This asymmetry is postulated to be due to the magnetic reconnection in the leading hemisphere of Ganymede that accelerates plasma toward Ganymede's surface [*Khurana et al.*, 2007]. These correlations and their associated asymmetries are still an open question and are examined here.

Ganymede's magnetospheric environment has been studied before using theoretical and numerical MHD simulations where the formation of a magnetopause, magnetotail, and Alfvén wings were examined, which have broadened our knowledge and understanding of the plasma interaction with Ganymede [*Neubauer*, 1998; *Kopp and Ip*, 2002; *Ip and Kopp*, 2002; *Paty and Winglee*, 2004, 2006; *Paty et al.*, 2008; *Jia et al.*, 2008, 2009, 2010; *Duling et al.*, 2014; *Dorelli et al.*, 2015; *Tóth et al.*, 2016]. We use, for the first time, a three-dimensional self-consistent hybrid model (kinetic ions and fluid electrons) to examine the kinetic ion effects of the Jovian plasma interaction with Ganymede's magnetosphere to understand Ganymede's surface brightness pattern. First, we present the global effects of plasma interaction with Ganymede using our hybrid model and validate our simulation results through comparison with Galileo magnetometer observations. Then, we provide a global map of plasma precipitation to the surface of Ganymede and the energy distribution of precipitating Jovian plasma. Finally, we examine the effects of OCFL boundaries and magnetic reconnection on Ganymede's surface brightness pattern when Ganymede is in the Jovian plasma sheet.

2. Model

We use a three-dimensional self-consistent hybrid model of plasma, where ions are treated as particles, and electrons are a massless charge-neutralizing fluid. The electric field, **E**, derived from the electron momentum equation is given by

$$\mathbf{E} = \frac{1}{\rho_i}(-\mathbf{J}_i \times \mathbf{B} + \mathbf{J} \times \mathbf{B} - \nabla p_e) + \eta \mathbf{J}, \tag{1}$$

where ρ_i and $\mathbf{J}_i$ are the charge and current densities of all particle ions, respectively, **J** is the total current density obtained from Ampere's law, p_e is a scalar electron pressure, and η is the resistivity. Faraday's law is used to advance the magnetic field in time as $\partial \mathbf{B}/\partial t = -\nabla \times \mathbf{E}$. The model is described in detail in *Holmström et al.* [2012] and *Holmström* [2013] and previously has been used to study plasma interaction with the Moon [e.g., *Holmström et al.*, 2012; *Poppe et al.*, 2014; *Fatemi et al.*, 2015a], lunar magnetic anomalies [*Fatemi et al.*, 2015b; *Poppe et al.*, 2016], Mars [*Holmström and Wang*, 2015], and Callisto [*Lindkvist et al.*, 2015].

We use a Ganymede-centered Cartesian coordinate system, known as "GphiO." In this system, the $+x$ axis is along the Jovian plasma flow direction, the $+y$ axis is along the Ganymede-Jupiter vector and points toward Jupiter, and the z axis is parallel to the spin axis of Ganymede [*Kivelson et al.*, 2002]. We use a regular-spaced Cartesian grid with cubic cell size $\Delta L = R_G/10 \approx 0.5\delta_i$, where $R_G = 2630$ km is the radius of Ganymede and $\delta_i \approx 450$ km is the ion inertial length for the mean ion mass of 14.0 amu at Ganymede's orbit [*Kivelson et al.*, 2004]. We assume Ganymede is a perfect plasma absorber without an ionosphere and has an internal magnetic dipole with magnetic moment strength $|\mathbf{m}| \simeq 1.3 \times 10^{20}$ A·m^2, which provides a surface equatorial magnetic field magnitude of ~750 nT [*Kivelson et al.*, 1996]. In our model, plasma resistivity is zero and to handle the vacuum regions formed in our simulations we use a vacuum resistivity of $\eta = 0.5 \times 10^7 \Omega$·m (i.e., very low conductivity), as explained by *Holmström* [2013]. The vacuum resistivity is dynamically assigned to the grid cells whenever their density goes below $0.001 n_0$, where n_0 is the upstream plasma density.

We perform our hybrid simulation runs based on simulation parameters listed in *Jia et al.* [2008, Table 2], which are inferred from the Galileo's six close encounters (i.e., G1, G2, G7, G8, G28, and G29). We use a single plasma specie with mean mass 14.0 amu, singly charged, and we use a flow velocity of $140\hat{x}$ km/s for all of our simulations. In contrast to the simulation parameters used by *Jia et al.* [2008], we only include the thermal component of the Jovian plasma. Including energetic particles in a hybrid plasma model requires taking extremely small time steps, which would be computationally very expensive, and for the case of Ganymede is not currently possible. Therefore, we use plasma density $n_0 = 4$ cm^{-3} and $T_i = T_e = 200$ eV for the G8 flyby, with slightly higher temperature than the average thermal plasma temperature (i.e., ~60–100 eV) [*Kivelson et al.*, 2004] in order to approximate the effects of high-energy particles, and $n_0 = 3$ cm^{-3} and $T_i = T_e = 100$ eV otherwise. We present simulation results after they have reached steady state conditions ($t > 120$ s).

Furthermore, in order to calculate the high-resolution spatial distribution of precipitating ions onto Ganymede's surface, we have used the background electric and magnetic fields from the hybrid model to trace ions from the upstream boundary through the model until each ion either struck Ganymede or left the simulation. Each ion trajectory is advanced in time at $\Delta t = 0.05\Omega_g^{-1}$, where Ω_g is the instantaneous ion gyrofrequency. If an ion strikes the surface of Ganymede, we record the local flux in a two-dimensional grid covering Ganymede's longitude and latitude. We have individually simulated H^+, O^{++}, and S^{+++} ions ranging from energies of 1 keV to 10^4 keV in $10^{0.25}$ sized logarithmic bins. While the thermal Jovian plasma consists of singly charged protons and oxygen [*Kivelson et al.*, 2004], the energetic component of Jupiter's magnetospheric particles is dominated mainly by a combination of H^+, O^{++}, and S^{+++} [*Collier and Hamilton*, 1995; *Keppler and Krupp*, 1996; *Mauk et al.*, 2004]. Whereas the thermal Jovian plasma contain the bulk of the flux at Ganymede's orbit [*Kivelson et al.*, 2004], the energetic particle spectrum (i.e., $E \gtrsim 10$ keV) is thought to be the main driver for particle surface weathering, i.e., radiolysis and neutral sputtering [*Johnson*, 1990; *Shi et al.*, 1995; *Baragiola et al.*, 2013]. Thus, we focus on the energetic particle population for the particle-tracing model. To absolutely normalize the flux of incident energetic particles, we use the distributions for each species as determined by *Mauk et al.* [2004] from Galileo Energetic Particle Detector (EPD) data for the G8 flyby specifically. For each specific pair of ion composition and energy, we have simulated $>10^8$ particles to ensure sufficient statistics.

3. Results

Figure 1 shows a snapshot of our hybrid simulation results for the G8 flyby when Ganymede is located in the Jovian plasma sheet. Figures 1a and 1b show the normalized magnetic field magnitude ($|\mathbf{B}|/|\mathbf{B}_0|$, where $|\mathbf{B}_0| = 77.3$ nT for the G8 flyby) in the *xz* and *yz* planes, respectively. As shown by the magnetic field streamlines, the closed field line regions at low latitudes near the equator and open field line regions at high latitudes in the polar caps are evident. Figure 1a shows the Alfvén wings form and bend the open field lines at Ganymede's polar caps with respect to the background Jovian magnetic fields. The magnetopause forms upstream of Ganymede at $\sim 2R_G$ from the center of Ganymede (Figure 1a) and the width of Ganymede's magnetosphere predicted by our model is $\sim 5.5R_G$ (Figure 1b), both of which are consistent with previous MHD simulations [e.g., *Paty and Winglee*, 2006; *Jia et al.*, 2009].

Figures 1c and 1d show the normalized plasma density (n/n_0, where $n_0 = 4$ cm^{-3}). The plasma density increases slightly upstream of Ganymede due to compressional waves propagating upstream and considerably decreases inside Ganymede's magnetosphere, which indicates the role that Ganymede's closed field lines play in shielding Ganymede's low latitudes from the incident Jovian plasma. In contrast, the density increases dramatically inside the Alfvén wings and over the polar caps to maintain the conservation of mass and density, concurrent with plasma deceleration in those regions. This density enhancement is in contrast with *Tóth et al.* [2016] simulations that show a large plasma cavity in the Alfvén wings.

Figures 1e–1g show the three components of plasma velocity (v_x, v_y, and v_z, respectively), all normalized to the Jovian corotating plasma flow speed $v_0 = 140$ km/s. We see from Figure 1e that the presence of Ganymede and its magnetosphere slows down the incident Jovian plasma upstream of Ganymede by ~25%, which is consistent with observations [*Williams et al.*, 1998] and MHD simulations [e.g., *Jia et al.*, 2008; *Dorelli et al.*, 2015]. We also see that the plasma flow velocity considerably decreases in the Alfvén wings and drops to nearly 20% of the corotating plasma speed near the surface at high latitudes, consistent with Galileo observations and analysis [*Williams et al.*, 1998; *Vasyliūnas and Eviatar*, 2000]. Additionally, plasma is accelerated toward the surface of Ganymede at the OCFL boundaries on the trailing hemisphere as well as on the leading hemisphere possibly due to magnetic reconnection upstream and downstream of Ganymede.

Figure 1f shows that the Jovian plasma is accelerated along the magnetic field lines toward the surface of Ganymede at the OCFL boundaries. However, we see from Figure 1d that the plasma density at the magnetic field separatix is very low. Figure 1g shows plasma acceleration along the background Jovian fields at the magnetopause and magnetotail. The white lines in Figure 1g are the streamlines of the plasma flow that indicate the flow diversion around Ganymede's magnetosphere. Finally, the field aligned currents (FACs) in the *yz* plane are shown in Figure 1h. These currents bend the magnetic field lines and contribute to the formation of the Alfvén wings.

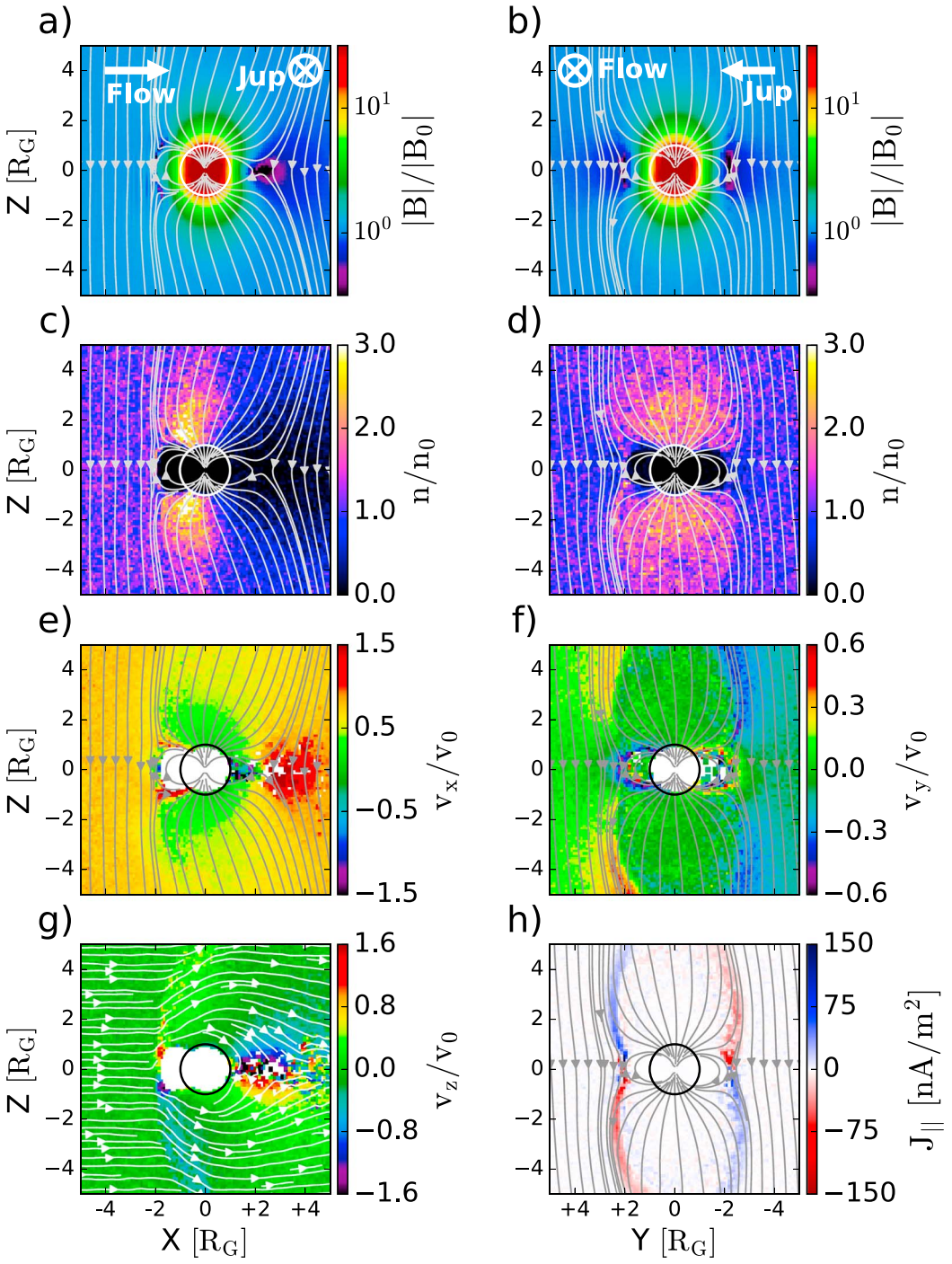

Figure 1. Hybrid simulation results during Galileo's G8 flyby presented in GphiO coordinate system. (a, b) magnitude of the magnetic field normalized to the background Jovian magnetic field B_0 = 77.3 nT, (c, d) plasma density normalized to the corotating plasma density n_0 = 4 cm^{-3}, (e–g) plasma velocity components along the *x*, *y*, and *z* axes, respectively, and normalized to the corotating plasma speed, v_0 = 140 km/s, and (h) field aligned current density. Streamlines show the magnetic field line tracing in all panels, except for panel g which shows the plasma flow vectors. Figures 1a, 1c, 1e, and 1g are cuts in the *xz* plane at *y*=0, viewed toward Jupiter, and Figures 1b, 1d, 1f, and 1h are cuts in the *yz* plane at *x*=0. Ganymede is shown by a circle, centered at the origin of the coordinate system, and the plasma flow direction and the location of Jupiter in each of the panels are shown by arrows.

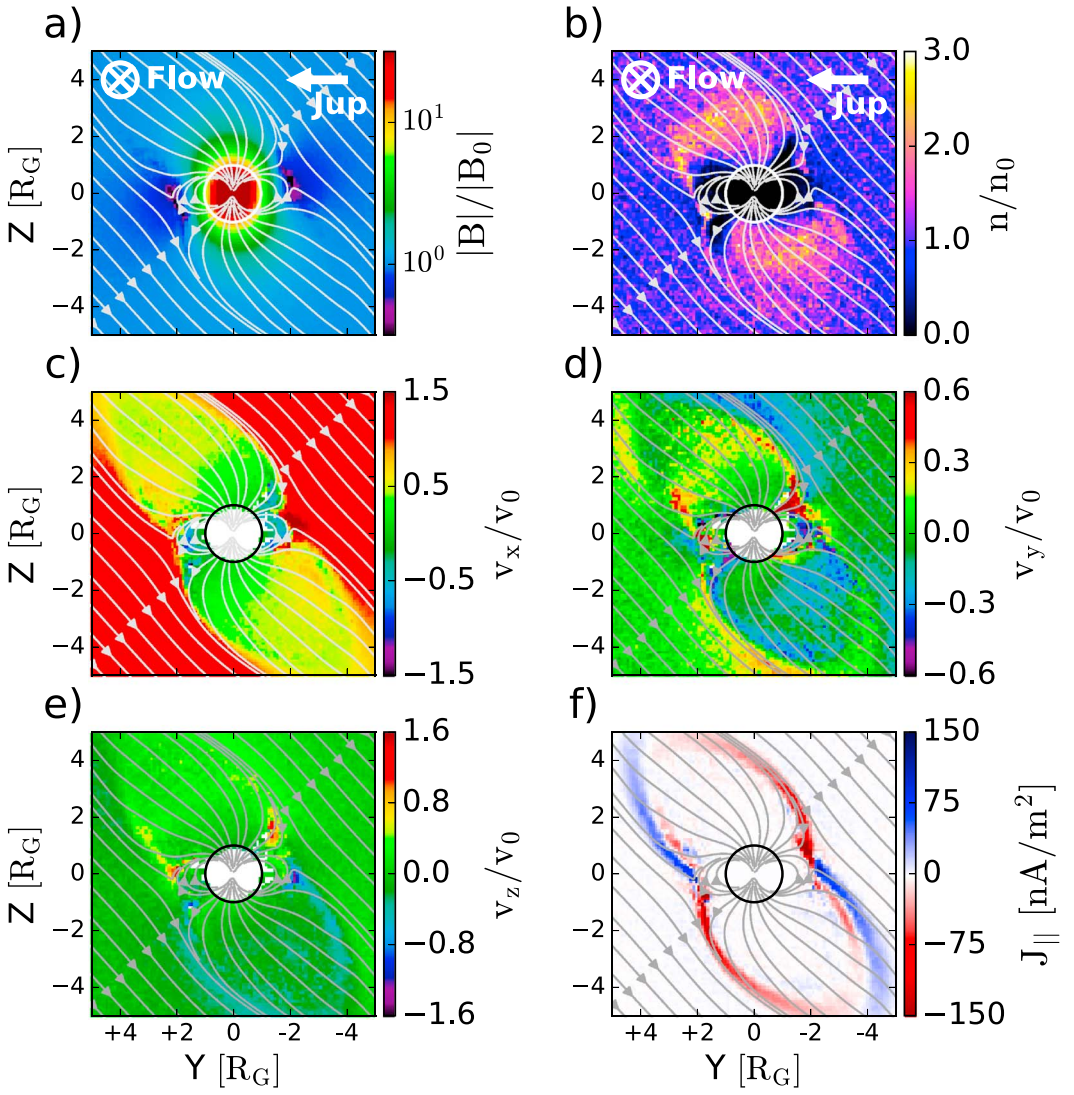

Figure 2. Hybrid simulation results during Galileo's G1 flyby presented in GphiO coordinate system. (a) magnitude of the magnetic field normalized to the background Jovian magnetic field B_0 = 111.7 nT, (b) plasma density normalized to the corotating plasma density n_0 = 3 cm^{-3}, (c–e) plasma velocity components along the *x*, *y*, and *z* axes, respectively, and normalized to the corotating plasma speed, v_0 = 140 km/s, (f) field aligned current density, in the *yz* plane at $x = 0$. The geometry of the cuts is the same as those in Figure 1.

Figure 2 shows our hybrid simulation results for the G1 flyby, as a representative of our simulations when Ganymede is outside the Jovian plasma sheet. The results are presented in the *yz* plane, perpendicular to the incident plasma flow. Despite the general differences in the Jovian magnetic field and plasma parameters between the G1 and G8 flybys, the overall conclusions drawn from our G8 simulation results and presented in Figure 1 hold for G1. These conclusions include plasma density enhancement inside the Alfvén wings and above the polar caps (Figure 2b), plasma deceleration inside the open field lines (Figure 2c), plasma acceleration toward Ganymede at the OCFL boundaries (Figure 2d), and the development of the FACs that form the Alfvén wings (Figure 2f).

Figure 3 compares the magnetic fields between our hybrid simulations (red lines) and Galileo magnetometer observations (blue lines) along the trajectories of the six Galileo flybys. There is a good agreement between our simulations and Galileo observations, particularly for the G1, G2, G28, and G29 flybys. For the G7 flyby (Figure 3c), other than B_x, the components agree well with observations. The mismatch for B_x may be due to a higher corotating plasma speed that we have used for this simulation (140 km/s) compared to that listed in *Jia et al.* [2008, Table 2] (130 km/s). Our simulation results for G8 (Figure 3d) have captured the overall trends

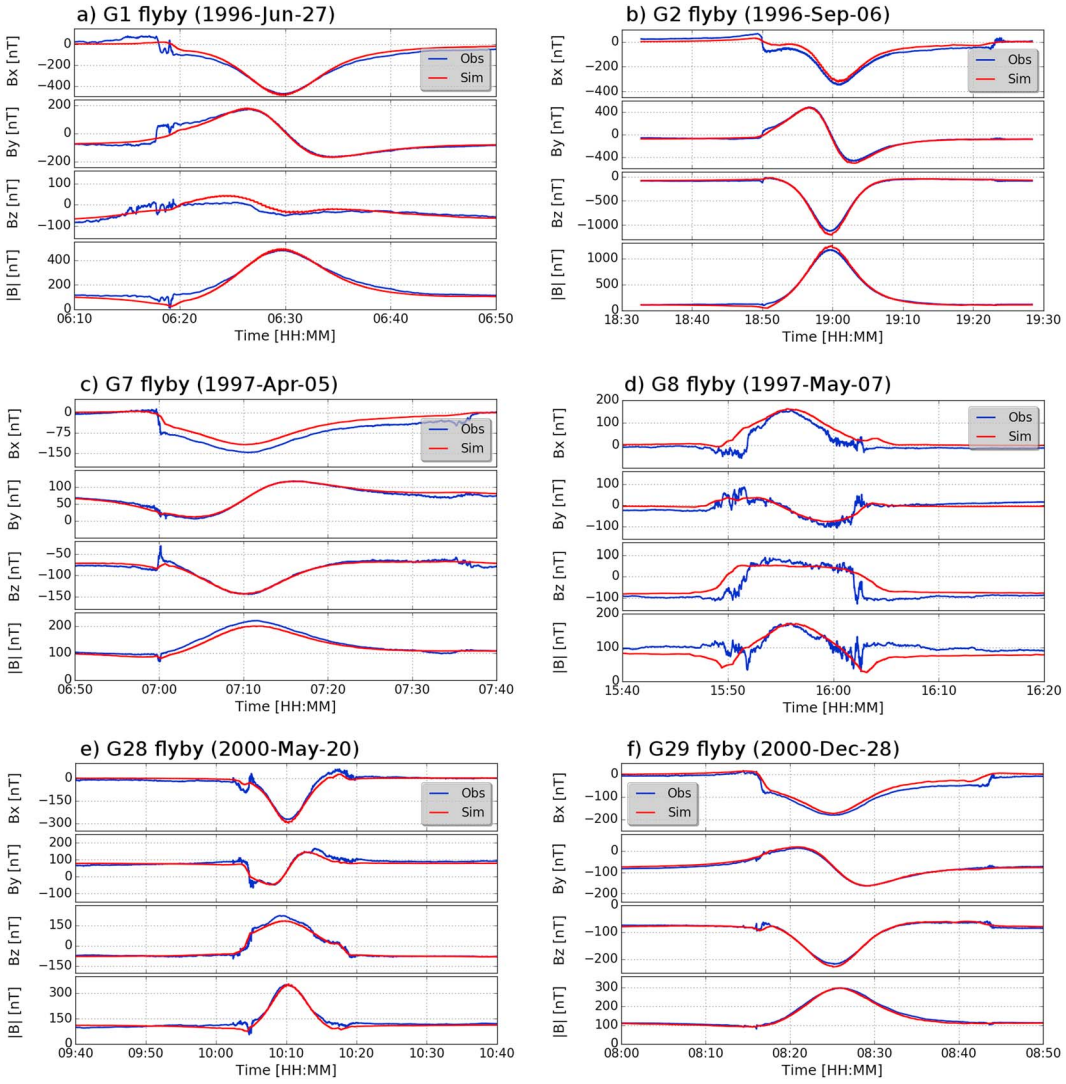

Figure 3. Magnetic field comparison between hybrid model simulations (red lines) and Galileo magnetometer observations (blue lines) for the six Galileo close flybys of Ganymede.

of the Galileo magnetic field observations, but the width of Ganymede's magnetosphere in our simulations is slightly broader than that shown in the Galileo data. This might be due to the omission of energetic particles in our hybrid simulations. Energetic particles carry considerable pressure in the plasma sheet, where the G8 flyby took place [*Mauk et al.*, 1996, 2004]. This high-energy particle pressure may cause additional compression of Ganymede's magnetosphere.

Figure 4a shows the total energetic particle flux precipitating to the surface of Ganymede predicted by our model when Ganymede is in the Jovian plasma sheet (i.e., G8 flyby). The superimposed dashed lines, taken from *McGrath et al.* [2013], are the approximate location of the boundaries between the bright polar caps and dark low latitudes on the surface of Ganymede obtained from Galileo imaging of Ganymede's surface [*Khurana et al.*, 2007]. Our model shows that a large flux of energetic particles precipitates to the high latitudes of Ganymede where the field lines are open, while the access of ions to the low latitudes is limited by the closed field lines. Moreover, there is a longitudinal asymmetry between the leading (0° – 180° longitude) and trailing (180° – 360° longitude) hemispheres at low latitudes near the equator (±30° latitude). Higher plasma flux impacts the surface of Ganymede at low latitudes in the leading hemisphere, possibly due to magnetic reconnection in Ganymede's magnetotail. Galileo surface imaging also shows a brighter leading hemisphere at low latitudes compared to the trailing hemisphere [*Khurana et al.*, 2007]. We see from Figure 4a that there is a good correlation between our model predicted plasma precipitation to the surface of Ganymede and Ganymede's

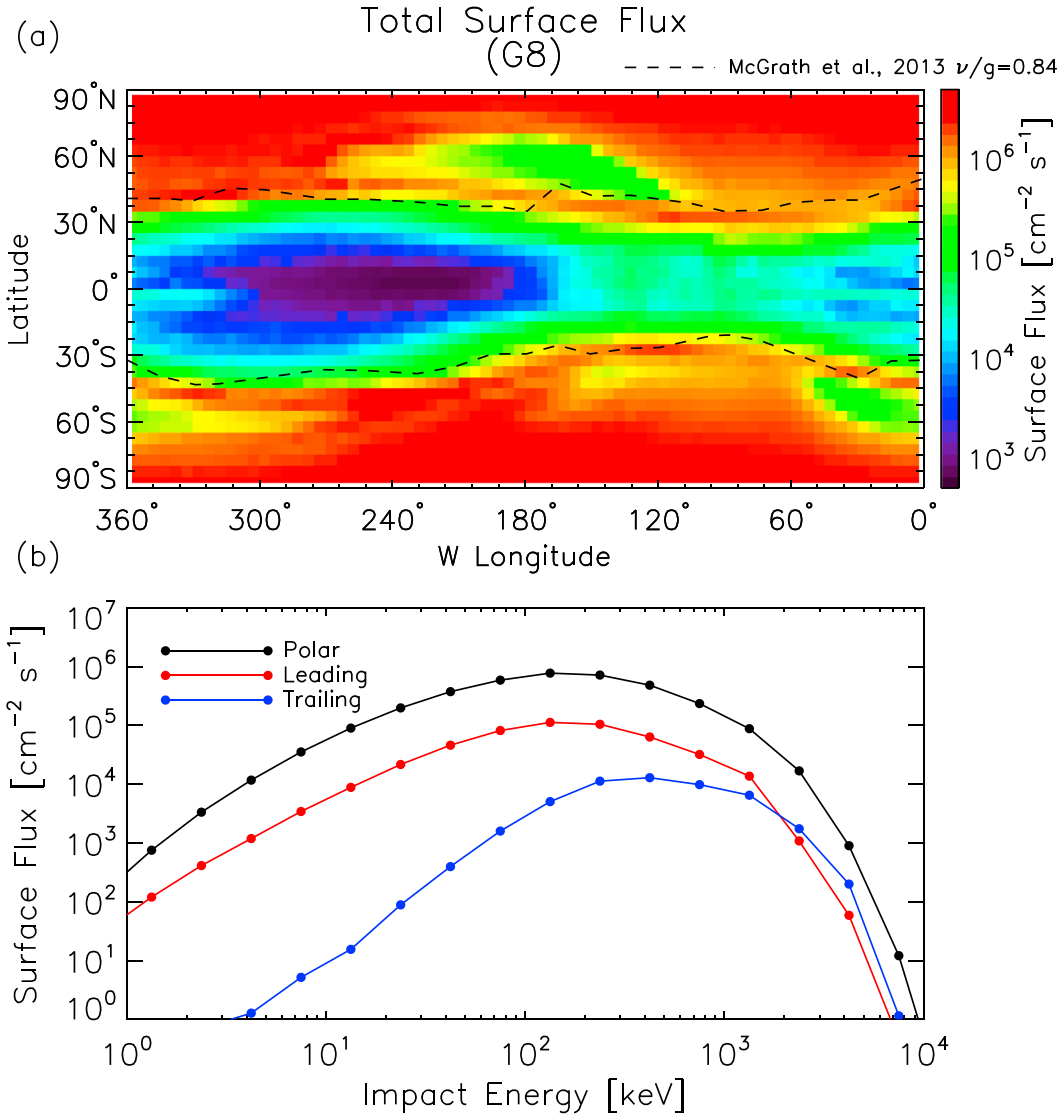

Figure 4. (a) The total flux of precipitating energetic ions to the surface of Ganymede from our model. The dashed lines taken from *McGrath et al.* [2013] are the violet-to-green ratio of 0.84 from the composite image of Ganymede's surface by *Khurana et al.* [2007] showing the approximate boundaries of Ganymede's bright polar caps and dark low latitudes. (b) Energy distribution for impacting Jovian energetic ion flux to the surface of Ganymede at the polar caps (black), leading (red), and trailing hemispheres (blue).

surface brightness pattern of *Khurana et al.* [2007], particularly at the Southern Hemisphere and the trailing side of the Northern Hemisphere. Small regions of reduced flux at high latitudes, for example, between ~40°N and 70°N at ~120°W–240°W, are mainly due to the tilt of Ganymede and Jovian magnetic dipoles during the G8 flyby. The average energetic ion flux during plasma sheet conditions, summed over all species and energies, to Ganymede's polar cap regions is approximately 3.6×10^6 cm^{-2} s^{-1} while the average ion flux to Ganymede's equatorial regions is roughly an order-of-magnitude less at approximately 1.4×10^5 cm^{-2} s^{-1}. These numbers compare favorably with previous estimates of the energetic ion flux to Ganymede's surface [*Cooper et al.*, 2001], noting that these previous estimates were made for G2 conditions.

In Figure 4b we show the energy distribution for incident energetic ions averaged within three distinct regions on the surface of Ganymede: polar caps (between 90°S–45°S and 45°N–90°N for all longitudes), low-latitude leading hemisphere (between 45°S–45°N and 0°W–180°W), and low-latitude trailing hemisphere (between 45°S–45°N and 180°W–360°W). The energy distributions of the incident ion flux on the polar cap (black) and leading hemisphere (red) peak at ~100 keV, while the trailing hemisphere distribution (blue) peaks at

~300 keV. We also see the variability of the impacting energy distribution at different regions as well as the asymmetry between the trailing and leading hemispheres. The main mechanism driving the reduction in fluxes for energies <200 keV, especially on the trailing hemisphere, is the presence of Ganymede's strong intrinsic magnetic fields, which shields Ganymede's surface from low-energy ions.

4. Discussion

We used a three-dimensional hybrid plasma model to study the Jovian plasma interaction with the magnetosphere and surface of Ganymede. Similar to single fluid and multifluid MHD simulations [e.g., *Paty and Winglee*, 2004; *Jia et al.*, 2009; *Dorelli et al.*, 2015], our hybrid simulation results presented in Figures 1 and 2 captured the global aspects of plasma interaction with Ganymede including formation of the magnetopause, magnetotail, Alfvén wings, flow diversion around Ganymede's magnetosphere, and magnetic reconnection upstream and downstream of Ganymede.

In our model, we only included a single plasma specie and we did not include Ganymede's ionosphere by any means, i.e., injecting ionospheric plasma [e.g., *Paty and Winglee*, 2004; *Paty et al.*, 2008] or including a conductive ionospheric boundary layer [e.g., *Jia et al.*, 2008, 2009; *Duling et al.*, 2014]. Yet our model results presented in Figure 3 are in good agreement with Galileo magnetic field observations. This suggests that Ganymede's ionosphere does not significantly distort Ganymede's strong intrinsic magnetic field. However, an ionosphere does have a critical contribution to Ganymede's aurora and associated electric field formation [*McGrath et al.*, 2013; *Saur et al.*, 2015], which requires further investigation beyond the scope of this research. Due to the lack of a conductive ionosphere in our model, the FACs in our hybrid simulations, in contrast to MHD simulations [*Jia et al.*, 2008, 2009; *Dorelli et al.*, 2015], do not close through the conductive ionosphere. Thus, there are no FACs at the OCFL boundaries in Figures 1h and 2f. The currents, however, close through the magnetopause in our model, which is not shown here. This demonstrates the role that including the ionosphere or conductive boundary layer play in the FAC closure.

Despite previous statements for the need to use very high resolution simulation grids to improve the correlation between Galileo observations and MHD simulations [*Paty and Winglee*, 2006; *Jia et al.*, 2008, 2009; *Dorelli et al.*, 2015], our hybrid simulation results show that even with relatively large grid sizes (only two cubic grid cells per ion inertial length compared to at least five in resistive and Hall MHD) [e.g., *Paty and Winglee*, 2006; *Jia et al.*, 2009; *Dorelli et al.*, 2015], a kinetic model is able to capture the physics of plasma interaction with Ganymede and provides good agreements with observations. Furthermore, in contrast to some previous MHD [i.e., *Jia et al.*, 2008; *Dorelli et al.*, 2015] and MHD-EPIC simulations [i.e., *Tóth et al.*, 2016], we neither shifted the Galileo spacecraft trajectory to match simulations with observations nor used an anomalous resistivity to force magnetic reconnection to take place. We do note that *Jia et al.* [2009, 2010], and *Duling et al.* [2014] achieved a good agreement between their MHD simulations and Galileo magnetic field observations without shifting the trajectory of Galileo by applying different boundary conditions.

Khurana et al. [2007] have used a superposition of Ganymede and Jupiter magnetic field models of *Kivelson et al.* [2002] and *Khurana* [1997] to examine the correlation between Ganymede's surface brightness and the OCFL boundaries. They found this correlation imperfect due to several potential reasons, including but not limited to, the lack of including higher order moments of the internal magnetic field of Ganymede and effects of Ganymede's inductive response on the OCFL boundaries in their model [*Khurana et al.*, 2007]. Moreover, their model did not include the self-consistent effects of the Jovian plasma on Ganymede's magnetic fields and their associated electric fields and currents that, for example, bend the magnetic fields in the Alfvén wings. In addition, *Plainaki et al.* [2015] provided a precipitation map for Jovian O^+ at a single initial energy (10 keV) and two different boundary conditions, which do not show a perfect correlation with surface brightness features. Here by using a particle-tracing model and electric and magnetic fields from our self-consistent hybrid model, we calculated the flux of precipitating energetic ions to the surface of Ganymede, presented in Figure 4a, and found good agreement between Ganymede's surface brightness and plasma precipitation to the surface. We also calculated the incident energy distribution of the energetic ion flux to the surface of Ganymede (Figure 4b). We found that the impacting ion flux generally peaks at ~100–300 keV. While the polar caps enable access of plasma to the surface of Ganymede (black line in Figure 4b), the closed field lines shield the low-energy part of the incident energy distribution on the trailing hemisphere (blue line in Figure 4b). In contrast, magnetic reconnection in the leading hemisphere enables impact of a broad energy range of the Jovian plasma on the leading hemisphere near the equator (red line in Figure 4b). Our model not only explains

the contrast between high- and low-latitude surface brightness but also explains the asymmetry between the leading and trailing hemispheres at low latitudes similar to that noted in imaging data [*Clark et al.*, 1986; *Calvin et al.*, 1995; *Khurana et al.*, 2007]. Our results support the conclusion that the leading-trailing asymmetry is most probably due to plasma acceleration toward the surface of Ganymede from magnetic reconnection in Ganymede's magnetotail. Similar surface brightness asymmetries between the leading and trailing hemispheres of Europa have also been reported [e.g., *McEwen*, 1986; *Sack et al.*, 1992]. The results of this study have important implications for our understanding of energetic particle surface weathering of icy moons, particularly Ganymede, Europa, and Callisto.

Acknowledgments
S.F. and A.R.P. acknowledge partial support from NASA's Solar System Workings program, grant NNX15AL20G. This research was conducted using resources provided by the Swedish National Infrastructure for Computing (SNIC) at the High Performance Computing Center North (HPC2N), Umeå University, Sweden, and supercomputers at Space Sciences Laboratory, UC Berkeley. The software used in this work was developed in part by the DOE NNSA ASC- and DOE Office of Science ASCR-supported Flash Center for Computational Science at the University of Chicago. All Galileo data used here are publicly available at NASA's Planetary Data System (PDS).

References

Baragiola, R. A., M. A. Famá, M. J. Loeffler, M. E. Palumbo, U. Raut, J. Shi, and G. Strazzulla (2013), *The Science of Solar System Ices*, chap. Radiation Effects in Water Ice in the Outer Solar System, pp. 527–549, Springer, New York.

Calvin, W. M., R. N. Clark, R. H. Brown, and J. R. Spencer (1995), Spectra of the icy Galilean satellites from 0.2 to 5 μm: A compilation, new observations, and a recent summary, *J. Geophys. Res.*, *100*(E9), 19,041–19,048.

Carlson, R. W., J. C. Bhattacharyya, B. A. Smith, T. V. Johnson, B. Hidayat, S. A. Smith, G. E. Taylor, B. O'Leary, and R. T. Brinkmann (1973), An atmosphere on Ganymede from its occultation of SAO 186800 on 7 June 1972, *Science*, *182*(4107), 53–55.

Clark, R. N., F. P. Fanale, and M. J. Gaffey (1986), Surface composition of natural satellites, in *Natural Satellites*, edited by J. A. Burns and M. S. Matthews, pp. 437–491, Univ. of Arizona Press, Arizona.

Collier, M. R., and D. C. Hamilton (1995), The relationship between kappa and temperature in energetic ion spectra at Jupiter, *Geophys. Res. Lett.*, *22*(3), 303–306.

Cooper, J. F., R. E. Johnson, B. H. Mauk, H. B. Garrett, and N. Gehrels (2001), Energetic ion and electron irradiation of the Icy Galilean satellites, *Icarus*, *149*(1), 133–159.

Dorelli, J. C., A. Glocer, G. Collinson, and G. Tóth (2015), The role of the Hall effect in the global structure and dynamics of planetary magnetospheres: Ganymede as a case study, *J. Geophys. Res. Space Physics*, *120*, 5377–5392, doi:10.1002/2014JA020951.

Duling, S., J. Saur, and J. Wicht (2014), Consistent boundary conditions at nonconducting surfaces of planetary bodies: Applications in a new Ganymede MHD model, *J. Geophys. Res. Space Physics*, *119*, 4412–4440, doi:10.1002/2013JA019554.

Eviatar, A., A. F. Cheng, C. Paranicas, B. H. Mauk, R. W. McEntire, and D. J. Williams (1998), Plasma flow in the magnetosphere of Ganymede, *Geophys. Res. Lett.*, *25*(8), 1257–1260.

Eviatar, A., V. M. Vasyliūnas, and D. A. Gurnett (2001), The ionosphere of Ganymede, *Planet. Space Sci.*, *49*(3–4), 327–336.

Fatemi, S., H. A. Fuqua, A. R. Poppe, G. T. Delory, J. S. Halekas, W. M. Farrell, and M. Holmström (2015a), On the confinement of lunar induced magnetic fields, *Geophys. Res. Lett.*, *42*, 6931–6938, doi:10.1002/2015GL065576.

Fatemi, S., C. Lue, M. Holmström, A. R. Poppe, M. Wieser, S. Barabash, and G. T. Delory (2015b), Solar wind plasma interaction with Gerasimovich lunar magnetic anomaly, *J. Geophys. Res. Space Physics*, *120*, 4719–4735, doi:10.1002/2015JA021027.

Frank, L. A., W. R. Paterson, K. L. Ackerson, and S. J. Bolton (1997), Outflow of hydrogen ions from Ganymede, *Geophys. Res. Lett.*, *24*(17), 2151–2154.

Gurnett, D. A., W. S. Kurth, A. Roux, S. J. Bolton, and C. F. Kennel (1996), Evidence for a magnetosphere at Ganymede from plasma-wave observations by the Galileo spacecraft, *Nature*, *384*(6609), 535–537.

Hall, D. T., P. D. Feldman, M. A. McGrath, and D. F. Strobel (1998), The far-ultraviolet oxygen airglow of Europa and Ganymede, *Astrophys. J.*, *499*(1), 475–481.

Holmström, M. (2013), Handling vacuum regions in a hybrid plasma solver, *ASTRONUM-2012, ASP Conf. Ser.*, *474*, 202–207.

Holmström, M., and X.-D. Wang (2015), Mars as a comet: Solar wind interaction on a large scale, *Planet. Space. Sci.*, *119*, 43–47.

Holmström, M., S. Fatemi, Y. Futaana, and H. Nilsson (2012), The interaction between the Moon and the solar wind, *Earth Planets Space*, *64*(2), 237–245.

Ip, W., and A. Kopp (2002), Resistive MHD simulations of Ganymede's magnetosphere 2. Birkeland currents and particle energetics, *J. Geophys. Res.*, *107*(A12), 1491, doi:10.1029/2001JA005072.

Jia, X., R. J. Walker, M. G. Kivelson, K. K. Khurana, and J. A. Linker (2008), Three-dimensional MHD simulations of Ganymede's magnetosphere, *J. Geophys. Res.*, *113*, A06212, doi:10.1029/2007JA012748.

Jia, X., R. J. Walker, M. G. Kivelson, K. K. Khurana, and J. A. Linker (2009), Properties of Ganymede's magnetosphere inferred from improved three-dimensional MHD simulations, *J. Geophys. Res.*, *114*, A09209, doi:10.1029/2009JA014375.

Jia, X., R. J. Walker, M. G. Kivelson, K. K. Khurana, and J. A. Linker (2010), Dynamics of Ganymede's magnetopause: Intermittent reconnection under steady external conditions, *J. Geophys. Res.*, *115*, A12202, doi:10.1029/2010JA015771.

Johnson, R. E. (1990), *Energetic Charged-Particle Interactions With Atmospheres and Surfaces*, Springer, New York.

Johnson, R. E. (1997), Polar "caps" on Ganymede and Io revisited, *Icarus*, *128*(2), 469–471.

Keppler, E., and N. Krupp (1996), The charge state of helium in the Jovian magnetosphere: A possible method to determine it, *Planet. Space Sci.*, *44*(2), 71–75.

Khurana, K. K. (1997), Euler potential models of Jupiter's magnetospheric field, *J. Geophys. Res.*, *102*, 11,295–11,306.

Khurana, K. K., R. T. Pappalardo, N. Murphy, and T. Denk (2007), The origin of Ganymede's polar caps, *Icarus*, *191*, 193–202.

Kivelson, M. G., K. K. Khurana, C. T. Russell, R. J. Walker, J. Warnecke, F. V. Coroniti, C. Polanskey, D. J. Southwood, and G. Schubert (1996), Discovery of Ganymede's magnetic field by the Galileo spacecraft, *Nature*, *384*(6609), 537–541.

Kivelson, M. G., J. Warnecke, L. Bennett, S. Joy, K. K. Khurana, J. A. Linker, C. T. Russell, R. J. Walker, and C. Polanskey (1998), Ganymede's magnetosphere: Magnetometer overview, *J. Geophys. Res.*, *103*, 19,963–19,972.

Kivelson, M. G., K. K. Khurana, and M. Volwerk (2002), The permanent and inductive magnetic moments of Ganymede, *Icarus*, *157*(2), 507–522.

Kivelson, M. G., F. Bagenal, W. S. Kurth, F. M. Neubauer, C. Paranicas, and J. Saur (2004), Magnetospheric interactions with satellites, in *Jupiter: The Planet, Satellites and Magnetosphere*, pp. 513–536, Cambridge Univ. Press, Cambridge, U. K.

Kopp, A., and W. Ip (2002), Resistive MHD simulations of Ganymede's magnetosphere 1. Time variabilities of the magnetic field topology, *J. Geophys. Res.*, *107*(A12), 1490, doi:10.1029/2001JA005071.

Lindkvist, J., M. Holmström, K. K. Khurana, S. Fatemi, and S. Barabash (2015), Callisto plasma interactions: Hybrid modeling including induction by a subsurface ocean, *J. Geophys. Res. Space Physics*, *120*(6), 4877–4889, doi:10.1002/2015JA021212.

Mauk, B. H., S. A. Gary, M. Kane, E. P. Keath, S. M. Krimigis, and T. P. Armstrong (1996), Hot plasma parameters of Jupiter's inner magnetosphere, *J. Geophys. Res.*, *101*(A4), 7685–7695.
Mauk, B. H., D. G. Mitchell, R. W. McEntire, C. P. Paranicas, E. C. Roelof, D. J. Williams, S. M. Krimigis, and A. Lagg (2004), Energetic ion characteristics and neutral gas interactions in Jupiter's magnetosphere, *J. Geophys. Res.*, *109*, A09S12, doi:10.1029/2003JA010270.
McEwen, A. S. (1986), Exogenic and endogenic albedo and color patterns on Europa, *J. Geophys. Res.*, *91*(B8), 8077–8097.
McGrath, M. A., X. Jia, K. Retherford, P. D. Feldman, D. F. Strobel, and J. Saur (2013), Aurora on Ganymede, *J. Geophys. Res. Space Physics*, *118*, 2043–2054, doi:10.1002/jgra.50122.
Neubauer, F. M. (1998), The sub-Alfvénic interaction of the Galilean satellites with the Jovian magnetosphere, *J. Geophys. Res.*, *103*(E9), 19,843–19,866.
Paty, C., and R. Winglee (2004), Multi-fluid simulations of Ganymede's magnetosphere, *Geophys. Res. Lett.*, *31*, L24806, doi:10.1029/2004GL021220.
Paty, C., and R. Winglee (2006), The role of ion cyclotron motion at Ganymede: Magnetic field morphology and magnetospheric dynamics, *Geophys. Res. Lett.*, *33*, L10106, doi:10.1029/2005GL025273.
Paty, C., W. Paterson, and R. Winglee (2008), Ion energization in Ganymede's magnetosphere: Using multifluid simulations to interpret ion energy spectrograms, *J. Geophys. Res.*, *113*, A06211, doi:10.1029/2007JA012848.
Plainaki, C., A. Milillo, S. Massetti, A. Mura, X. Jia, S. Orsini, V. Mangano, E. De Angelis, and R. Rispoli (2015), The H_2O and O_2 exospheres of Ganymede: The result of a complex interaction between the Jovian magnetospheric ions and the icy moon, *Icarus*, *245*, 306–319.
Poppe, A. R., S. Fatemi, J. S. Halekas, M. Holmström, and G. T. Delory (2014), ARTEMIS observations of extreme diamagnetic fields in the lunar wake, *Geophys. Res. Lett.*, *41*(11), 3766–3773.
Poppe, A. R., S. Fatemi, I. Garrick-Bethell, D. Hemingway, and M. Holmström (2016), Solar wind interaction with the Reiner Gamma crustal magnetic anomaly: Connecting source magnetization to surface weathering, *Icarus*, *266*, 261–266.
Sack, N., R. Johnson, J. Boring, and R. Baragiola (1992), The effect of magnetospheric ion bombardment on the reflectance of Europa's surface, *Icarus*, *100*(2), 534–540.
Saur, J., et al. (2015), The search for a subsurface ocean in Ganymede with Hubble Space Telescope observations of its auroral ovals, *J. Geophys. Res. Space Physics*, *120*, 1715–1737, doi:10.1002/2014JA020778.
Shi, M., R. A. Baragiola, D. E. Grosjean, R. E. Johnson, S. Jurac, and J. Schou (1995), Sputtering of water ice surfaces and the production of extended neutral atmospheres, *J. Geophys. Res.*, *100*(E12), 26,387–26,395.
Smith, B. A., et al. (1979), The Galilean satellites and Jupiter: Voyager 2 imaging science results, *Science*, *206*(4421), 927–950.
Tóth, G., et al. (2016), Extended magnetohydrodynamics with embedded particle-in-cell simulation of Ganymede's magnetosphere, *J. Geophys. Res.*, *121*, 1273–1293, doi:10.1002/2015JA021997.
Vasyliūnas, V. M., and A. Eviatar (2000), Outflow of ions from Ganymede: A reinterpretation, *Geophys. Res. Lett.*, *27*(9), 1347–1349.
Volwerk, M., M. G. Kivelson, K. K. Khurana, and R. L. McPherron (1999), Probing Ganymede's magnetosphere with field line resonances, *J. Geophys. Res.*, *104*(A7), 14,729–14,738.
Williams, D. J., B. Mauk, and R. W. McEntire (1998), Properties of Ganymede's magnetosphere as revealed by energetic particle observations, *J. Geophys. Res.*, *103*, 17,523–17,534.